

# UNet-AF: An alias-free UNet for image restoration

Jérémy Scanvic<sup>1,2</sup>

jeremy.scanvic@ens-lyon.fr

Quentin Barthélemy<sup>2</sup>

q.barthelemy@hirschsecure.fr

Julián Tachella<sup>1</sup>

julian.tachella@ens-lyon.fr

<sup>1</sup> Laboratoire de Physique de l'ENS de Lyon, CNRS, Lyon, France <sup>2</sup> Hirsch, Lyon, France

**Abstract**—The simplicity and effectiveness of the UNet architecture makes it ubiquitous in image restoration, image segmentation, and diffusion models. They are often assumed to be equivariant to translations, yet they traditionally consist of layers that are known to be prone to aliasing, which hinders their equivariance in practice. To overcome this limitation, we propose a new alias-free UNet designed from a careful selection of state-of-the-art translation-equivariant layers. We evaluate the proposed equivariant architecture against non-equivariant baselines on image restoration tasks and observe competitive performance with a significant increase in measured equivariance. Through extensive ablation studies, we also demonstrate that each change is crucial for its empirical equivariance<sup>1</sup>.

**Index Terms**—UNet, Translation-Equivariance, Aliasing

## I. INTRODUCTION

UNet networks are encoder-decoder neural networks that operate across multiple scales using pairs of pooling/downsampling and upsampling layers, and have concatenation layers bridging the encoder and decoder at each scale. Notably, they are commonly applied in medical imaging [1], [2], in image super-resolution [3] and in diffusion models [4].

In many applications, UNet networks are expected to be equivariant to translations, i.e., that their output translates with their input. To do so, they typically rely on the building blocks of convolutional neural networks (CNN) [5].

However, recent work shows that standard CNNs are only approximately equivariant to translations, mostly due to aliasing in pooling and upsampling layers [6]–[8]. They propose to combine pooling and upsampling layers with anti-aliasing filters to reduce aliasing, and thus increase approximate equivariance.

Chaman and Dokmanić [9] identify activation functions as another source of aliasing, which hinders translation-equivariance. They introduce adaptive pooling and upsampling whereby the sampling grid shifts with the input, thereby recovering perfect equivariance to whole-pixel translations. However, this solution does not improve equivariance to sub-pixel (continuous) translations [10].

Karras *et al.* [11] emphasize the importance of sub-pixel equivariance for image generation to avoid texture sticking and reframe the problem using a traditional approach built upon sampling theory. Discrete finite images are viewed as representations of bandlimited periodic images related through sampling and Whittaker-Shannon (sinc) interpolation [12]. Instead of using adaptive sampling, they reduce the aliasing caused by activation functions by low-pass filtering them. They

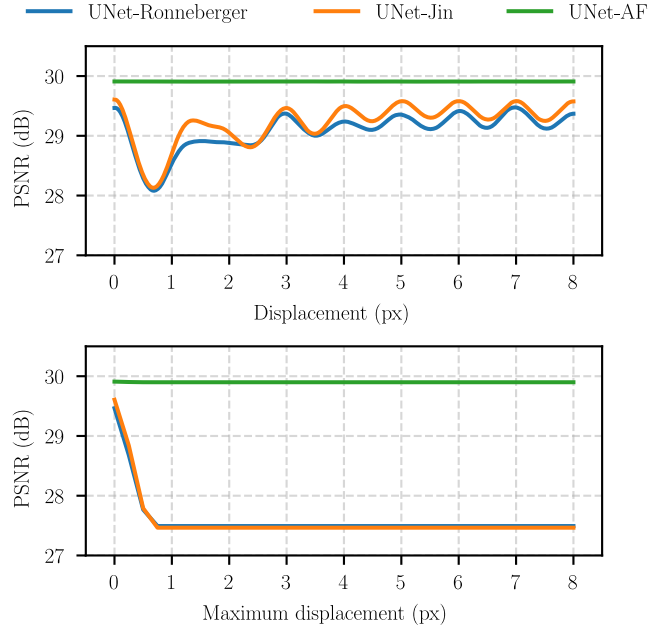


Fig. 1. **Equivariance and robustness to circular translations.** (Top) Performance on a horizontally translated image, with 0.01 px steps, (bottom) adversarial performance on the worst translation up to a maximum displacement, with 0.25 px steps. UNet-AF is stable and robust, unlike the baselines.

also advocate for the use of anti-aliasing filters with a sharper cut-off, and a flatter response in the pass and stop bands, although more computationally expensive.

Michaeli *et al.* [10] go one step further and use exact sinc filters implemented using the fast Fourier transform (FFT). They also identify the lack of smoothness of ReLU as a cause of aliasing and substitute it for polynomial activations, and propose an alias-free substitute to layer normalization.

Despite having been applied successfully to classifiers (encoder type) [10], [13], and image generators (decoder type) [11], layers equivariant to continuous sub-pixel translations remain, to the best of our knowledge, to be applied to encoder-decoder architectures including UNet architectures.

Our contributions are the following:

- We propose a new alias-free UNet architecture (UNet-AF) using state-of-the-art translation-equivariant layers.
- We evaluate its effectiveness, training stability, computational efficiency, and empirical equivariance on multiple image restoration tasks.
- We conduct extensive ablation studies to validate its design, and identify its tradeoffs.

<sup>1</sup>Our implementation is available at <https://github.com/jscanvic/UNet-AF>

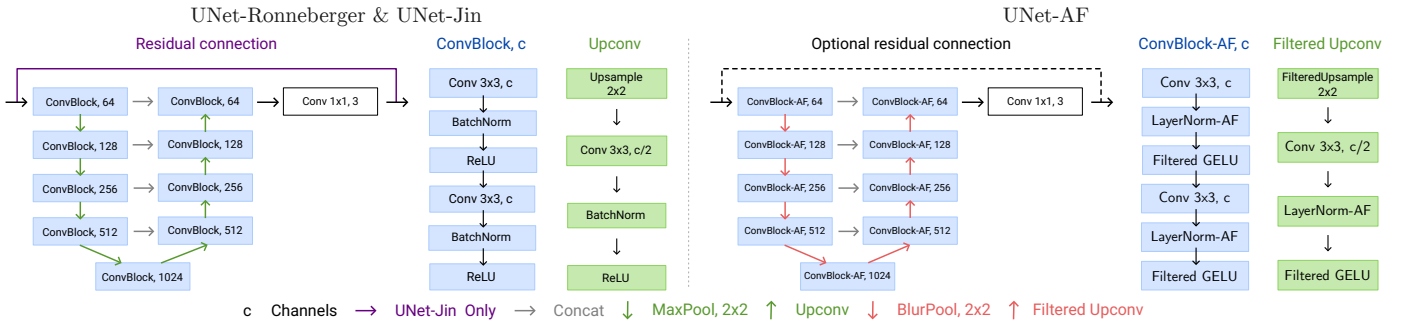


Fig. 2. **Overview of the architecture.** UNet-AF is obtained by changing the architectures of Ronneberger *et al.* [1] and Jin *et al.* [2]. Anti-aliasing filters are added in upsampling layers, max pooling layers are replaced with blur pooling layers, ReLU activations are replaced with filtered GELU layers and batch normalization is replaced by alias-free layer normalization. The padding mode in convolutions is left unconstrained and the residual connection is optional.

## II. ALIAS-FREE UNET

Our proposed architecture is based on that of Jin *et al.* [2] (UNet-Jin) which features an additional residual connection on top of the architecture of Ronneberger *et al.* [1] (UNet-Ronneberger). This base architecture is not translation-equivariant, and we apply a series of modifications to render it equivariant. While we focus on this specific UNet, our analysis can be easily applied to other UNet backbones. In this section, we discuss every layer type used in the base architecture, i.e., convolutions, residual connections, concatenation layers, pooling layers, upsampling layers, activation functions, and normalization layers, presenting the necessary changes to obtain a translation-equivariant counterpart.

Formally, a discrete image  $x \in \mathbb{R}^n$  is interpolated as  $\varphi * x$  where  $\varphi$  is the continuous sinc function and  $*$  denotes circular convolution [11], [12]. Sampling the convolution of a translated version of  $\varphi$  with  $x$  on the original grid yields the translation of  $x$  denoted as  $T_g x$  where  $g \in \mathbb{R}^2$  is the displacement. In this setting, translation-equivariance is expressed as

$$f(T_g x) = T_g f(x), \quad \forall x \in \mathbb{R}^n, \quad \forall g \in \mathbb{R}^2, \quad (1)$$

where  $f$  denotes the UNet.

*a) Convolutions:* While convolutions are not prone to aliasing, a mismatch in padding mode with the translations causes boundary errors, and thus a loss of equivariance. Therefore, we use circular convolutions for circular translations, and zero-padded convolutions for crop-translations [7].

*b) Residual connections:* The original architecture features a global residual connection, and while it does not introduce aliasing, we find that it is not always beneficial to performance and training stability. It is made optional in UNet-AF, and it is enabled when it is measurably beneficial to performance.

*c) Concatenation layers:* Intermediate concatenation layers are present in the base architecture, sometimes referred to as skip connections. These do not introduce aliasing, and they remain present in the UNet-AF architecture.

*d) Pooling layers:* We substitute max-pooling for blur pooling with periodic sinc anti-aliasing implemented using the FFT, similarly to Michaeli *et al.* [10]. Due to the contribution

of every input pixel to each output pixel, this anti-aliasing scheme is more computationally costly than the filters used by Zhang [7], Chaman and Dokmanić [9], and Karras *et al.* [11], including the box filter used in average pooling, and windowed sinc filtering. Instead, it eliminates aliasing within numerical precision, which results in higher equivariance. We use this anti-aliasing consistently in other layers.

*e) Upsampling layers:* The original upsampling scheme consists in merely inserting zeros between input pixels, which preserves input information in the output low-frequencies, yet fills the high-frequencies with aliasing. It is eliminated in the proposed architecture using an anti-aliasing filter.

*f) Activation functions:* We replace ReLU activations with filtered activation functions [10], [11], which consist in first resampling the input on a finer grid, applying a base activation function, removing the high-frequencies, and resampling on the coarse grid. Instead of corrupting the output, part of the aliasing is removed with the high-frequencies, thereby improving equivariance. The upsampling rate is set to two, following previous work.

The GELU function is chosen as the underlying base activation function, similarly to Michaeli and Soudry [13]. Its smoothness limits the addition of high-frequencies in the finest grid, which improves equivariance, and unlike polynomial activations [10], its linear growth prevents it from amplifying numerical equivariance error.

*g) Normalization layers:* Scanvic *et al.* [14] show theoretically and empirically that batch normalization, instance normalization, and alias-free layer-normalization [10] are equivariant to translations, but standard layer normalization [15] is not. The batch normalization used in the original architecture is swapped for alias-free layer normalization in UNet-AF, for reasons of training stability and performance.

The final architecture is represented in Figure 2, and extensive experiments are conducted to evaluate it in the next section.

## III. EXPERIMENTS

We evaluate the UNet-AF architecture introduced in Section II by training it, along with two other UNet architectures [1], [2], to solve various imaging tasks, and by comparing

TABLE I

**PERFORMANCE ON CIRCULAR DEBLURRING.** THE CHANGES IN SECTION II LEAD TO A STEADY INCREASE IN EQUIVARIANCE (EQUIV), STABILIZE THE TRAINING DYNAMICS AND IMPROVE PERFORMANCE (PSNR, SSIM, LPIPS), AT THE EXPENSE OF HIGHER COMPUTATIONAL COST (FPS). BEST METRIC IN **BOLD**, SECOND BEST UNDERLINED. VALUES: AVG  $\pm$  ST.D.

Method	Difference	PSNR $\uparrow$	SSIM $\uparrow$	LPIPS $\downarrow$	EQUIV $\uparrow$	STAB $\uparrow$	FPS $\uparrow$
UNet-Ronneberger		31.28 $\pm$ 2.13	0.9316 $\pm$ 0.0271	0.0377 $\pm$ 0.0235	37.60 $\pm$ 2.62	9.10	<b>2494</b>
UNet-Jin	+ Res conn.	31.64 $\pm$ 2.51	0.9280 $\pm$ 0.0345	0.0402 $\pm$ 0.0254	38.20 $\pm$ 2.22	12.86	<u>2114</u>
	+ LayerNorm-AF	32.16 $\pm$ 2.37	0.9383 $\pm$ 0.0211	0.0355 $\pm$ 0.0210	38.41 $\pm$ 1.99	18.40	1230
	+ Circular pad.	<b>32.46 <math>\pm</math> 2.45</b>	<b>0.9417 <math>\pm</math> 0.0209</b>	<b>0.0323 <math>\pm</math> 0.0199</b>	43.16 $\pm$ 2.38	<u>20.63</u>	982
	+ Filtered GELU	32.22 $\pm$ 2.39	<u>0.9383 <math>\pm</math> 0.0201</u>	0.0331 $\pm$ 0.0193	43.55 $\pm$ 2.77	20.48	302
	+ Filtered Upconv.	<u>32.24 <math>\pm</math> 2.35</u>	0.9382 $\pm$ 0.0201	0.0333 $\pm$ 0.0197	<u>46.33 <math>\pm</math> 2.59</u>	20.34	293
UNet-AF	+ BlurPool	32.22 $\pm$ 2.32	0.9373 $\pm$ 0.0204	<u>0.0330 <math>\pm</math> 0.0210</u>	<b>81.63 <math>\pm</math> 0.26</b>	<b>20.81</b>	290
Blurred images		26.24 $\pm$ 2.30	0.8170 $\pm$ 0.0406	0.2258 $\pm$ 0.0719	N/A	N/A	N/A

the resulting models using various metrics. In Section III-A, we describe the different tasks in more detail, and we compare the performance of the three architectures, and in Section III-B we report extensive ablation studies on the proposed architecture.

For a fair comparison, the different models are trained using the same training procedure from the DeepInverse library [16]. It minimizes a mean squared error loss using Adam [17] with a learning rate of  $5e-4$ , a batch size of 5, and no weight decay.

The architectures are evaluated using two distortion metrics, the PSNR and SSIM [18], one perceptual metric, LPIPS [19], one equivariance metric, EQUIV [20], one training stability metric, STAB, and one metric of computational efficiency, FPS. Precisely, EQUIV is the average PSNR of the equivariance error associated to eq. (1), STAB is the standard deviation of the evaluation PSNR increments from one epoch to the next, and FPS is the average number of images processed in a second at inference, measured on a NVIDIA H100 GPU.

#### A. Image restoration

Three image restoration tasks are considered, 1) image deblurring with circular boundary conditions, 2) deblurring with cropped boundaries and 3) denoising. We pre-process the 900 natural images from DIV2K [21] to constitute our ground truths for training, which we further split into 700 training images, 100 evaluation images and 100 test images. Each image is first resized to 256 px and then its center 128 px are cropped so that information at the boundary is available to compute crop-translations similarly to Zhang [7].

For tasks 1) and 2), ground truth images are first blurred using a Gaussian filter with standard deviation 1 px. They are then further corrupted with additive white Gaussian noise with a standard deviation of 0.01, while for task 3) the filtering step is absent and the standard deviation is set to 0.1.

Image restoration consists in recovering high-quality images  $x_{HQ}$  from degraded images  $x_{LQ}$ . In our experiments, we consider settings with blur and noise

$$x_{LQ} = h * x_{HQ} + \varepsilon \quad (2)$$

where  $h$  denotes a Gaussian blur kernel and  $\varepsilon$  is additive white Gaussian noise. We train each UNet to directly map degraded images to high-quality images. As long as the degradation

TABLE II

**PERFORMANCE ON ADDITIONAL TASKS.** WE EVALUATE UNET-AF ON VALID DEBLURRING, AND GAUSSIAN DENOISING. BEST METRIC IN **BOLD**, SECOND BEST UNDERLINED. VALUES: AVG  $\pm$  ST.D.

Method	Task	PSNR $\uparrow$	EQUIV $\uparrow$
UNet-Ronneberger	Valid deblurring	31.67 $\pm$ 2.33	39.96 $\pm$ 2.71
UNet-Jin		<u>32.25 <math>\pm</math> 2.41</u>	<u>42.82 <math>\pm</math> 2.96</u>
UNet-AF		<b>32.30 <math>\pm</math> 2.42</b>	<b>46.57 <math>\pm</math> 2.58</b>
Blurred images		26.85 $\pm$ 2.55	N/A
UNet-Ronneberger	Gaussian denoising	<b>29.70 <math>\pm</math> 1.56</b>	39.80 $\pm$ 1.31
UNet-Jin		29.58 $\pm$ 1.61	<u>40.64 <math>\pm</math> 1.78</u>
UNet-AF		<u>29.66 <math>\pm</math> 1.57</u>	<b>78.96 <math>\pm</math> 1.44</b>
Noisy images		20.00 $\pm$ 0.03	N/A

process is equivariant to translations, which is the case for uniform blur and additive white Gaussian noise, it suffices that the network is equivariant to render the whole system equivariant [20], [22]

$$f(h * (T_g x_{HQ}) + T_g \varepsilon) = T_g f(h * x_{HQ} + \varepsilon). \quad (3)$$

We use different variants of the UNet-AF depending on the specific task. For circular deblurring and denoising, we use circular padding, and for valid deblurring, we use zero-padding. Moreover, the residual connection is present for deblurring tasks, but not for denoising, for improved performance and training stability.

Table I shows that the changes in Section II result in a steady increase in equivariance from UNet-Ronneberger and UNet-Jin to UNet-AF, with a significant final difference of about 40 dB. Moreover, our architecture is both more performant and more stable at training than the two baselines.

Table II shows the results on valid deblurring, and we observe that UNet-AF is slightly more equivariant to crop-translations as well than UNet-Ronneberger and UNet-Jin. Unlike circular translations, these are not invertible as they discard and introduce information at the boundaries, and it is expected that the equivariance errors are greater. Moreover, UNet-AF is significantly more performant than the two baselines. The table also shows the results on the denoising task, and we observe that UNet-AF is significantly more equivariant than UNet-Ronneberger and UNet-Jin with similar values than



Fig. 3. Reconstructions of a circularly blurred image. The PSNR is displayed in the bottom-left corner of each image.

for the circular deblurring task. In this setting however, the three models have comparable performance.

Unlike the experiments of Michaeli *et al.* [10] on alias-free classifiers, we observe no significant drop in performance due to blur pooling, and neither for alias-free layer normalization which we find to significantly increase performance as well as training stability. However, we observe a slight drop in performance due to the filtered activation functions as well, and we believe that increasing the depth of the network might compensate for this change.

Inference speed is mostly hindered by the change in normalization and activation functions, with the final equivariant network being about 7 times slower than the starting implementation of UNet-Jin. The substitution of standard layers for alias-free alternatives is also detrimental to computational efficiency, which is explained by the presence of additional filters.

The difference in training stability is illustrated by Figure 4, which shows the validation PSNR for each epoch. Moreover, the difference in equivariance is illustrated by Figure 1, which shows the PSNR for an image translated by varying displacements on average (top), or adversarially (bottom). The noticeable phase change around 2 px translations is explained by the transition from an equivariance error dominated by boundary artifacts that only affect small translations, to a regime where the smaller aliasing error that is always present dominates. The deblurring performance is also shown on Figure 3 for one of the test images.

### B. Ablation studies

We assess the impact of each choice in Section II by evaluating the outcome of alternate options. Specifically, each model is trained on the circular deblurring task introduced in Section III-A, and Table III shows the results for each layer, including residual connections, normalization layers, padding in convolutions, activation functions, and upsampling and pooling layers.

We observe a drop of about 40 dB in equivariance when any of the layers is substituted for an alternative prone to aliasing, thereby showing that each change in Section II equally contributes to the equivariance of the final model. In this setting, we also observe a noticeable increase in performance for the variant with a residual connection.

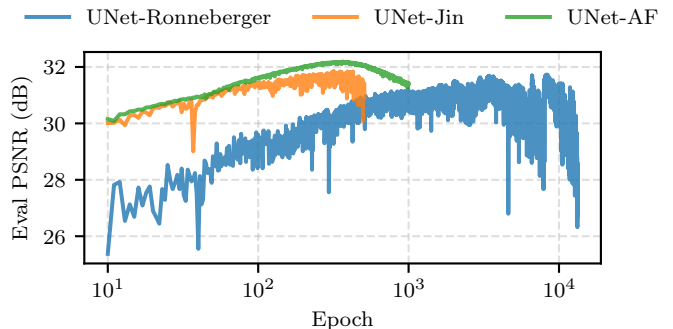


Fig. 4. Evaluation PSNR throughout training for circular deblurring. Our proposed model has significantly smoother training dynamics than the non-equivariant baselines.

TABLE III  
ABLATION STUDY. EACH DESIGN CHOICE MADE IN SECTION II IS EXPLORED IN TERMS OF PERFORMANCE AND EQUIVARIANCE. BEST METRIC IN **BOLD**, SECOND BEST UNDERLINED. VALUES: AVG  $\pm$  S.T.D.

Replacement	Variant	PSNR $\uparrow$	EQUIV $\uparrow$
Res. connection	Present	<b>32.22 <math>\pm</math> 2.32</b>	<b>81.63 <math>\pm</math> 0.26</b>
	Absent	<u>31.96 <math>\pm</math> 2.33</u>	<u>77.77 <math>\pm</math> 2.32</u>
Normalization	LayerNorm-AF	<u>32.22 <math>\pm</math> 2.32</u>	<u>81.63 <math>\pm</math> 0.26</u>
	BatchNorm	32.21 $\pm$ 2.31	80.62 $\pm$ 8.14
	InstanceNorm	31.50 $\pm$ 2.19	78.40 $\pm$ 0.42
	LayerNorm	<b>32.31 <math>\pm</math> 2.36</b>	54.19 $\pm$ 3.03
	None	32.10 $\pm$ 2.39	<b>84.78 <math>\pm</math> 3.91</b>
Padding	Circular	<b>32.22 <math>\pm</math> 2.32</b>	<b>81.63 <math>\pm</math> 0.26</b>
	Zeros	<u>32.14 <math>\pm</math> 2.36</u>	40.35 $\pm$ 1.95
	Reflect	32.09 $\pm$ 2.38	40.24 $\pm$ 2.10
Activation	Filtered GELU	32.22 $\pm$ 2.32	<b>81.63 <math>\pm</math> 0.26</b>
	GELU	<u>32.28 <math>\pm</math> 2.41</u>	47.03 $\pm$ 2.83
	Filtered ReLU	<b>32.28 <math>\pm</math> 2.35</b>	<u>78.95 <math>\pm</math> 1.21</u>
	ReLU	32.27 $\pm$ 2.42	45.38 $\pm$ 2.80
	Filtered Poly	26.29 $\pm$ 2.20	55.56 $\pm$ 0.86
Poly	26.25 $\pm$ 2.25	53.96 $\pm$ 0.95	
Upsampling	Filtered	<b>32.22 <math>\pm</math> 2.32</b>	<b>81.63 <math>\pm</math> 0.26</b>
	Unfiltered	<u>32.15 <math>\pm</math> 2.33</u>	<u>45.90 <math>\pm</math> 2.69</u>
Pooling	BlurPool	32.22 $\pm$ 2.32	<b>81.63 <math>\pm</math> 0.26</b>
	MaxPool	<u>32.24 <math>\pm</math> 2.35</u>	46.33 $\pm$ 2.59
	AvgPool	32.15 $\pm$ 2.36	46.59 $\pm$ 2.71
	MaxBlurPool	<b>32.32 <math>\pm</math> 2.40</b>	<u>47.03 <math>\pm</math> 3.10</u>

Despite being theoretically free of aliasing, we find that filtered polynomial activations measurably hinder equivariance. We believe that this error stems from the amplification of prior numerical error when it passes in the quadratic terms of activation layers. Moreover, unlike Michaeli *et al.* [10] but similarly to Michaeli and Soudry [13], we find that these layers result in a significant decrease in performance. As predicted in Section II, the use of filtered GELU instead of filtered ReLU as the base activation layer leads to slightly better equivariance.

We find that despite averaging neighboring pixel values, average pooling hinders equivariance as much as regular max pooling, which is consistent with the relatively low attenuation of box filters in the stop band. Moreover, despite having been proposed by Zhang [7] to improve the equivariance of CNNs, we find that MaxBlurPool is as poor as max pooling and blur pooling in terms of equivariance.

We find that, consistently with previous work [23], layer normalization is detrimental to equivariance, but that instance normalization, batch normalization and alias-free layer normalization are not. Moreover, we observe that instance normalization performs significantly worse than batch normalization and alias-free layer normalization, and that alias-free layer normalization performs slightly better than batch normalization. We also observe that removing the normalization layers altogether lead to only a small gain in equivariance, despite removing all of the numerical error they introduce, which shows that alias-free layer normalization is numerically close to optimal.

#### IV. CONCLUSION

We propose a new UNet architecture free of aliasing (UNet-AF) using state-of-the-art layers equivariant to continuous translations. We validate it extensively on image restoration tasks including circular and valid Gaussian deblurring and Gaussian denoising. We also conduct extensive ablation studies to validate our design choices and find that each of the substitutions we make is necessary for the overall equivariance of the network. Our experiments show that equivariance to translations tends to be correlated with performance and training stability, but at a greater computational expense. Nonetheless, there might be room for optimization using different anti-aliasing filters better optimized for specific layers, and a precise use of dedicated GPU kernels for these operations, which we leave for future work.

#### ACKNOWLEDGEMENTS

This project was provided with computing HPC and storage resources by GENCI at IDRIS thanks to the grant 2025-AD011016422 on the supercomputer Jean Zay's H100 partition.

#### REFERENCES

- [1] O. Ronneberger, P. Fischer, and T. Brox, "U-Net: Convolutional Networks for Biomedical Image Segmentation," in *MICCAI*, 2015.
- [2] K. H. Jin, M. T. McCann, E. Froustey, and M. Unser, "Deep Convolutional Neural Network for Inverse Problems in Imaging," *IEEE Trans Image Process*, 2017.

- [3] K. Zhang, L. Van Gool, and R. Timofte, "Deep Unfolding Network for Image Super-Resolution," in *CVPR*, 2020.
- [4] K. Crowson, S. A. Baumann, A. Birch, T. M. Abraham, D. Z. Kaplan, and E. Shippole, "Scalable high-resolution pixel-space image synthesis with hourglass diffusion transformers," in *ICML*, 2024.
- [5] Y. Lecun, L. Bottou, Y. Bengio, and P. Haffner, "Gradient-Based Learning Applied to Document Recognition," *Proc IEEE*, 1998.
- [6] A. Azulay and Y. Weiss, "Why Do Deep Convolutional Networks Generalize so Poorly to Small Image Transformations?" *JMLR*, 2019.
- [7] R. Zhang, "Making Convolutional Networks Shift-Invariant Again," in *ICML*, 2019.
- [8] X. Zou, F. Xiao, Z. Yu, and Y. J. Lee, "Delving Deeper into Anti-aliasing in ConvNets," *IJCV*, 2023.
- [9] A. Chaman and I. Dokmanić, "Truly Shift-Equivariant Convolutional Neural Networks with Adaptive Polyphase Upsampling," in *ACSSC*, 2021.
- [10] H. Michaeli, T. Michaeli, and D. Soudry, "Alias-Free Convnets: Fractional Shift Invariance via Polynomial Activations," in *CVPR*, 2023.
- [11] T. Karras, M. Aittala, S. Laine, *et al.*, "Alias-Free Generative Adversarial Networks," in *NeurIPS*, 2021.
- [12] M. Vetterli, J. Kovačević, and V. K. Goyal, *Foundations of Signal Processing*. Cambridge Univ Press, 2014.
- [13] H. Michaeli and D. Soudry, "Alias-Free ViT: Fractional Shift Invariance via Linear Attention," in *NeurIPS*, 2025.
- [14] J. Scanvic, M. Davies, P. Abry, and J. Tachella, *Scale-Equivariant Imaging: Self-Supervised Learning for Image Super-Resolution and Deblurring*, 2025. arXiv: 2312.11232.
- [15] Z. Liu, H. Mao, C.-Y. Wu, C. Feichtenhofer, T. Darrell, and S. Xie, "A ConvNet for the 2020s," in *CVPR*, 2022.
- [16] J. Tachella, M. Terris, S. Hurault, *et al.*, "DeepInverse: A Python package for solving imaging inverse problems with deep learning," *JOSS*, 2025.
- [17] D. P. Kingma and J. Ba, *Adam: A Method for Stochastic Optimization*, 2017. arXiv: 1412.6980.
- [18] Z. Wang, A. Bovik, H. Sheikh, and E. Simoncelli, "Image quality assessment: From error visibility to structural similarity," *IEEE Trans Image Process*, 2004.
- [19] R. Zhang, P. Isola, A. A. Efros, E. Shechtman, and O. Wang, "The Unreasonable Effectiveness of Deep Features as a Perceptual Metric," in *CVPR*, 2018.
- [20] V. Sechaud, J. Scanvic, Q. Barthélemy, P. Abry, and J. Tachella, "Equivariant Splitting: Self-supervised learning from incomplete data," in *ICLR*, 2026.
- [21] E. Agustsson and R. Timofte, "NTIRE 2017 Challenge on Single Image Super-Resolution: Dataset and Study," in *CVPRW*, 2017.
- [22] D. Chen, M. Davies, M. J. Ehrhardt, C.-B. Schönlieb, F. Sherry, and J. Tachella, "Imaging With Equivariant Deep Learning: From unrolled network design to fully unsupervised learning," *IEEE Signal Process Mag*, 2023.
- [23] J. Scanvic, Q. Barthélemy, and J. Tachella, "Translation-Equivariance of Normalization Layers and Aliasing in Convolutional Neural Networks," in *TASC*, 2025.